

## Spectroscopic diagnostics for ablation cloud of tracer-encapsulated solid pellet in LHD<sup>a)</sup>

N. Tamura,<sup>1</sup> V. Yu. Sergeev,<sup>2</sup> D. V. Kalina,<sup>1</sup> I. V. Miroshnikov,<sup>2</sup> K. Sato,<sup>1</sup> I. A. Sharov,<sup>2</sup> O. A. Bakhareva,<sup>2</sup> D. M. Ivanova,<sup>2</sup> V. M. Timokhin,<sup>2</sup> S. Sudo,<sup>1</sup> and B. V. Kuteev<sup>3</sup>

<sup>1</sup>National Institute for Fusion Science, 322-6, Oroshi-cho, Toki-City, Gifu 509-5292, Japan

<sup>2</sup>State Polytechnical University, Politechnicheskaya 29, St. Petersburg 195251, Russia

<sup>3</sup>Nuclear Fusion Institute, RRC "Kurchatov Institute," Kurchatov square 1, Moscow 123182, Russia

(Presented 15 May 2008; received 9 May 2008; accepted 22 June 2008; published online 31 October 2008)

In the Large Helical Device (LHD), various spectroscopic diagnostics have been applied to study the ablation process of an advanced impurity pellet, tracer-encapsulated solid pellet (TESPEL). The total light emission from the ablation cloud of TESPEL is measured by photomultipliers equipped with individual interference filters, which provide information about the TESPEL penetration depth. The spectra emitted from the TESPEL ablation cloud are measured with a 250 mm Czerny–Turner spectrometer equipped with an intensified charge coupled device detector, which is operated in the fast kinetic mode. This diagnostic allows us to evaluate the temporal evolution of the electron density in the TESPEL ablation cloud. In order to gain information about the spatial distribution of the cloud parameters, a nine image optical system that can simultaneously acquire nine images of the TESPEL ablation cloud has recently been developed. Several images of the TESPEL ablation cloud in different spectral domains will give us the spatial distribution of the TESPEL cloud density and temperature. © 2008 American Institute of Physics. [DOI: [10.1063/1.2957928](https://doi.org/10.1063/1.2957928)]

### I. INTRODUCTION

In the study of magnetically confined high temperature plasmas, an impurity injection has been utilized for a variety of purposes, such as to study impurity transport in the core plasma,<sup>1</sup> transient heat transport with the resultant cold pulse propagation,<sup>2</sup> and to improve the surface condition of the vacuum vessel.<sup>3</sup> As a method of injecting the impurity into the plasma, the pellet injection technique has been widely used. With this technique, the ablation characteristics of the pellet are also important issues to be clarified because those will determine the capability as a diagnostics tool as well as the pellet penetration depth.

In the Large Helical Device (LHD), a tracer-encapsulated solid pellet<sup>4</sup> (TESPEL) has been used for promoting the above-described studies. TESPEL is a double-layered impurity pellet, which consists of polystyrene polymer ( $\text{CH}(\text{C}_6\text{H}_5)\text{CH}_2$ ) as an outer shell (the typical diameter ranges from 0.5 to 0.9 mm) and tracer particles as an inner core (the typical size is 0.1–0.2 mm in size). The TESPEL is injected from the outboard side of LHD by means of a pneumatic pipe gun. Helium is used as the accelerating gas and its pressure is typically 35 atm. The resultant TESPEL velocity ranges from 200 to 500  $\text{m s}^{-1}$ , which is measured by using the time-of-flight method. One of the unique features of the TESPEL is that local deposition of the tracer particle can be achieved inside the core plasma. Thus, in the study with TESPEL injection, it is important to know

where the tracer is deposited inside the plasma as well as how deep the TESPEL penetrates into the plasma. In order to obtain such information and some physical parameters regarding the TESPEL ablation cloud, various spectroscopic diagnostic systems have been installed on LHD, as described below.

### II. TESPEL PENETRATION MONITOR

Figure 1 shows the field of view ( $9^\circ$ ) of a collimator lens with a diameter of 19 mm and a focal length of 30 mm in the collector optics as the TESPEL penetration monitor, together with the TESPEL injection axis. The collector optics are installed at the port adjacent to the TESPEL injection port. Both ports are on the equatorial plane of LHD. The light emission from the ablating TESPEL is received with the collector optics through a quartz window and a half mirror and then is transmitted to another room by an optical fiber with a core diameter of 0.8 mm and a numerical aperture of 0.2. In the other room, the ablation emission transmitted is bifurcated by using an optical fiber bundle, which consists of eight optical fibers, each with a core diameter of 0.23 mm, and is transmitted to a photomultiplier tube (PMT) system and a spectrometer, respectively. The ablation emission entering the PMT system is divided again by the half mirror, and each divided emission is detected by the PMT with a specified interference filter. The PMT signals are digitized with a sampling frequency of 1 MHz. In the case of using a titanium (Ti) tracer, one of the PMTs is equipped with an  $\text{H}_\alpha$  filter (center  $\lambda$ : 657.2 nm, bandwidth: 1.2 nm) for measuring

<sup>a)</sup>Contributed paper, published as part of the Proceedings of the 17th Topical Conference on High-Temperature Plasma Diagnostics, Albuquerque, New Mexico, May 2008.

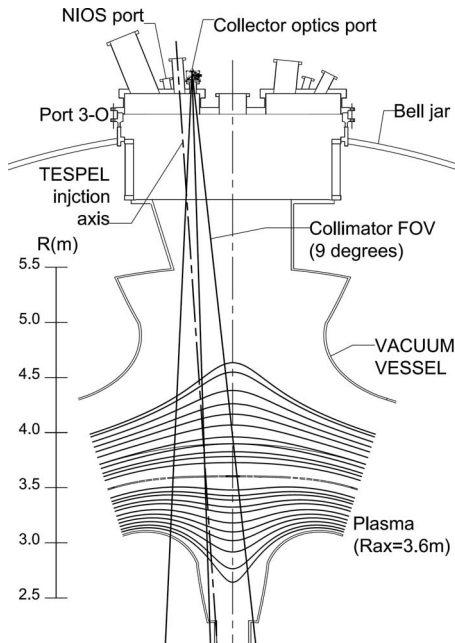


FIG. 1. Field of view of a collimator lens on the equatorial plane of LHD. The TESPEL injection axis is on that plane.

the shell ablation and the other is equipped with Ti I filter (center  $\lambda$ : 400.3 nm, bandwidth: 2.0 nm) for measuring the Ti tracer ablation.

Figure 2 shows typical examples of the PMT signals when the TESPEL with or without the Ti tracer is injected into the LHD plasma. The high time-resolved PMT signal is translated to the spatial profile of the ablation emission by using the measured TESPEL velocity. Thus the duration of the tracer ablation, which is indicated by the shaded area in Fig. 2(b), represents the deposition width of the tracer. In general, the electron temperature at the region where the tracer is exposed to the LHD plasma is so high (typically  $\sim 0.5$ – $1$  keV) that the ablation and ionization to higher charge states of the Ti tracer proceed very quickly and consequently the Ti I emission from the Ti tracer appears and

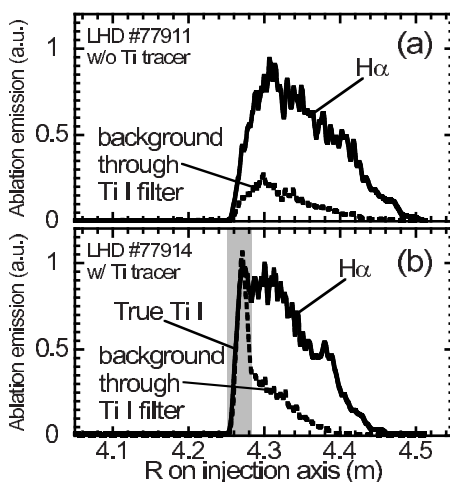


FIG. 2. Ablation emission measured with photomultipliers equipped with an  $H\alpha$  filter (solid lines) and a Ti I filter (dotted lines) as a function of the major radial position along the TESPEL injection axis for the cases (a) without and (b) with the titanium tracer.

disappears promptly. In the case of Fig. 2(b), the deposition width of the tracer is estimated to be about 3 cm. Thus the local deposition capability of the TESPEL is experimentally verified.

### III. HIGH TIME-RESOLVED MEASUREMENT OF ABLATION LIGHT SPECTRUM

A pellet charge exchange (PCX) diagnostic, which consists of the TESPEL and a neutral particle analyzer, has been utilized to investigate the behavior of fast ions in the LHD plasma.<sup>5</sup> The PCX diagnostic requires the knowledge of electron density, which would change with the TESPEL traveling across the plasma, in the TESPEL ablation cloud. In order to evaluate the electron density in the TESPEL ablation cloud, measurement of the Stark broadening of the Balmer- $\beta$  line emitted from the TESPEL ablation cloud is made, since the outer shell of TESPEL is made of CH polymer. The spectra emitted from the TESPEL ablation cloud are measured with a Czerny–Turner spectrometer (focal length: 250 mm,  $F/4.3$ ) coupled with an intensified charge coupled device (CCD) detector (Andor DH534-FK). In order to efficiently measure the width of the Balmer- $\beta$  ( $\lambda=486.14$  nm) line profile, the blazed wavelength of the grating with  $1200$  grooves  $\text{mm}^{-1}$  is set at  $1$   $\mu\text{m}$  to measure the second order of the Balmer- $\beta$ ,  $972.27$  nm. The bifurcated fiber bundle which consists of 4 optical fibers each with a core diameter of  $0.23$  mm is placed at the entrance slit of the spectrometer and the width of the slit is set to  $100$   $\mu\text{m}$ . The CCD chip consists of  $1024 \times 1024$  pixels and the effective pixel size is  $19.5$   $\mu\text{m}^2$ . As an operation mode, the fast kinetic mode is used in this measurement. The pixel height of the exposed area is 42 pixels and the vertical shift speed is specially tuned,  $2$   $\mu\text{s}$   $\text{row}^{-1}$ . The resultant exposure time of this system is  $84$   $\mu\text{s}$ . Thus, the instrument can provide multiple spectra during the TESPEL ablation, since the typical duration of the TESPEL ablation is  $\sim 1$  ms. The instrument function of this spectrometer at the second order of the Balmer- $\beta$  is measured with a hydrogen lamp, and it is approximated by the full width at half maximum (FWHM) of a Gaussian profile fitted to the measured Balmer- $\beta$  line profile. The FWHM of the fitted Gaussian profile is 11.89 pixels on the CCD chip, which corresponds to  $0.52$  nm at  $972.27$  nm. This instrument function is taken into account in determining the Stark width.

The electron density in the TESPEL cloud is evaluated from the FWHM of a Lorentzian profile fitted to the measured Balmer- $\beta$  line profile, together with the following relationship:  $n_e = \sqrt[1.04]{(2.38 \times 10^{21})(\Delta\lambda)^{3/2}}$ , where  $\Delta\lambda$  is FWHM. This relationship is derived from Griem's table.<sup>6</sup> In this relationship, any temperature effect is ignored.

In LHD No. 70910, at the time ( $t=1.438$  95 s) around when the spatially integrated Balmer- $\alpha$  line intensity measured with the PMT reaches a maximum value, the FWHM of the Balmer- $\beta$  line profile is  $3.78$  nm and thus the electron density in the TESPEL ablation cloud is evaluated as  $7.1 \times 10^{22}$   $\text{m}^{-3}$ , as shown in Fig. 3.

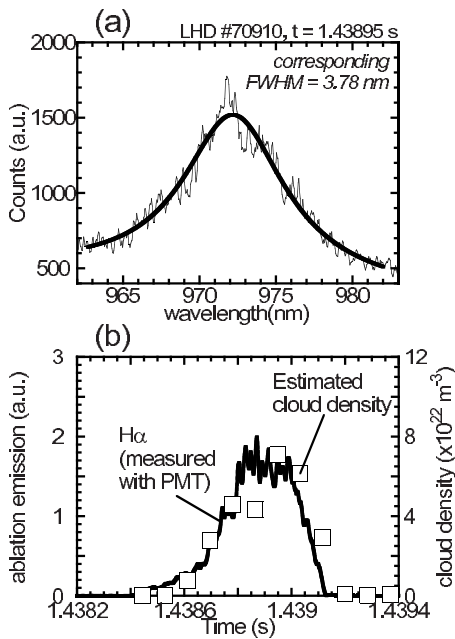


FIG. 3. (a) Line profile of Balmer- $\beta$  emission from the TESPEL ablation cloud (thin line) at  $t=1.43895$  s in LHD No. 70910 and the fitted Lorentzian profile (thick line). (b) Temporal evolution of the cloud density estimated from the fitted Lorentzian profiles (open square) together with the Balmer- $\alpha$  emission measured with the PMT (solid line). In this case, no tracer is contained in the TESPEL.

#### IV. NINE IMAGE OPTICAL SYSTEM (NIOS)

In order to gain information about the spatial distribution of the cloud parameters, a NIOS that can simultaneously acquire nine images of the TESPEL ablation cloud has recently been developed. Figure 4(a) shows a schematic side view of the NIOS. The NIOS consists of nine identical lenses (a diameter of 10 mm, a focal length of 190 mm), each of which is equipped with an individual aperture and an interference filter, a field lens (diameter of 53 mm, focal length of 75 mm), and a 12 bit compact digital camera with a fast shutter [PCO Pixelfly (Scientific specifications)], which is housed in a light shield black box. The 12 bit compact digital camera consists of a  $1280 \times 1024$  CCD with  $6.7 \mu\text{m}$  square pixels, which is equipped with an objective lens (Canon PHF12 1.4, a focal length of 12 mm,  $F/1.4$ ). The exposure time of the CCD camera can be set within the range of  $10 \mu\text{s}$ – $10$  s; typically  $10 \mu\text{s}$  is used to catch the time-sliced ablation cloud of the TESPEL. The installation port for the NIOS is adjacent to the TESPEL injection port as well as for the collector optics, as already shown in Fig. 1. Prior to the experiment, the following calibrations have been performed; sensitivity of each pixel to white uniform source, positioning and geometry transformations between nine images, and spectral sensitivity of pixels with and without the filters. Based on the results, normalization coefficients between each pixel are obtained, which are within  $\pm 50\%$  relative to their average values.

Figure 4(b) shows an example picture taken by the NIOS with the exposure time of  $10 \mu\text{s}$ . This picture shows the luminous clouds in six different spectral ranges in the early stage of the ablation, each of which is slightly tilted. The angle of tilt would correspond to that of magnetic field lines

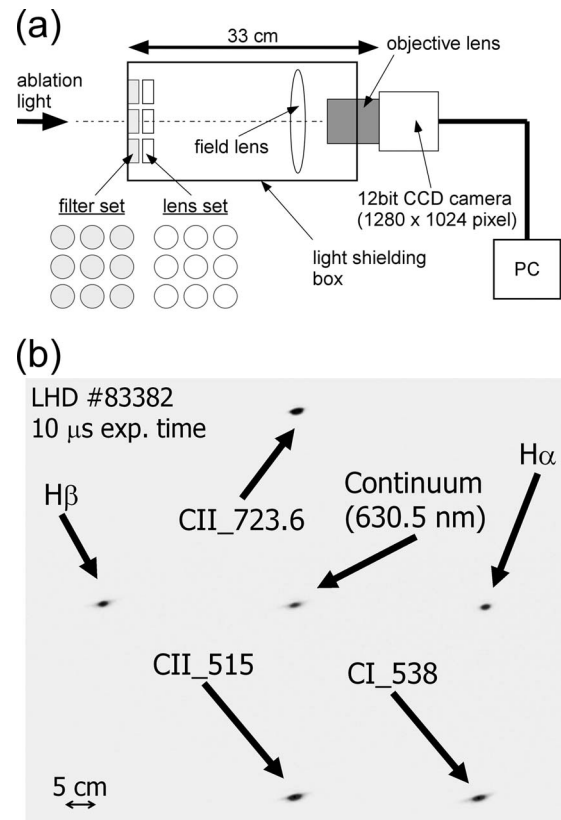


FIG. 4. (a) Schematic side view of the NIOS. (b) Example image taken by the NIOS. The image is taken with an exposure time of  $10 \mu\text{s}$ .

at the region where the picture is taken. From this picture, the electron temperature in the cloud can be estimated roughly by using the line (Balmer- $\alpha$ ,  $\beta$ )-to-continuum intensity ratio method,<sup>6</sup> assuming that local thermodynamic equilibrium (LTE) is established in the cloud. The electron temperature deduced here in the core region of the cloud is about 5 eV. More exact estimation of the electron temperature in the cloud will be performed after the verification of the LTE existence.<sup>7</sup> In order to measure the spatial distribution of the electron density in the TESPEL ablation cloud, the spatial distribution of the width of the Balmer- $\beta$  line profile, which is broadened dominantly by Stark broadening, is required. To this end, nine interference filters, each of which has a very slightly different center wavelength (nevertheless, it is near the Balmer- $\beta$  line, 486.14 nm) and bandwidth, will be installed.

#### ACKNOWLEDGEMENTS

The authors acknowledge all of the technical staff of NIFS for their excellent support. They also would like to thank Professor O. Motojima (Director of NIFS) for his continuous encouragement. This work is partly supported by a Grant-in-Aid for Scientific Research (B) (No. 19340179) from Japan Society for the Promotion of Science, and a Grant-in-Aid for Young Scientist (B) (No. 19740349) from MEXT Japan and a budgetary Grant-in-Aid No. NIFS07ULHH510 and NIFS07KEIN1018 of the National Institute for Fusion Science.

- <sup>1</sup>N. Tamura, S. Sudo, K. V. Khlopenkov, S. Kato, V. Yu. Sergeev, S. Muto, K. Sato, H. Funaba, K. Tanaka, T. Tokuzawa, I. Yamada, K. Narihara, Y. Nakamura, K. Kawahata, N. Ohyabu, O. Motojima, and LHD experimental group, *Plasma Phys. Controlled Fusion* **45**, 27 (2003).
- <sup>2</sup>N. Tamura, S. Inagaki, K. Tanaka, C. Michael, T. Tokuzawa, T. Shimozuma, S. Kubo, R. Sakamoto, K. Ida, K. Itoh, D. Kalinina, S. Sudo, Y. Nagayama, K. Kawahata, A. Komori, and LHD experimental group, *Nucl. Fusion* **47**, 449 (2007).
- <sup>3</sup>H. W. Kugel, M. G. Bell, R. Bell, C. Bush, D. Gates, T. Gray, R. Kaita, B. Leblanc, R. Maingi, R. Majeski, D. Mansfield, D. Mueller, S. Paul, R. Raman, A. L. Roquemore, S. Sabbagh, C. H. Skinner, V. Soukhanovskii, T. Stevenson, and L. Zakharov, *J. Nucl. Mater.* **363–365**, 791 (2007).
- <sup>4</sup>S. Sudo, *J. Plasma Fusion Res.* **69**, 1349 (1993).
- <sup>5</sup>P. R. Goncharov, T. Ozaki, S. Sudo, N. Tamura, TESPEL Group, LHD Experimental Group, E. A. Veshchev, V. Yu. Sergeev, and A. V. Krasilnikov, *Rev. Sci. Instrum.* **77**, 10F119 (2006).
- <sup>6</sup>H. R. Griem, *Spectral Line Broadening by Plasma* (Academic, New York, 1974).
- <sup>7</sup>M. Goto, R. Sakamoto, and S. Morita, *Plasma Phys. Controlled Fusion* **49**, 1163 (2007).